Processing and Application of Ceramics 18 [1] (2024) 77–86
https://doi.org/10.2298/PAC2401077C

In situ mullite whisker network formation for high strength and lightweight ceramic proppants

Xudong Chen[1,*], Saisai Li[1], Yudong Shang[2], Jun Wang[1], Jiaojiao Zheng[1]

[1]*Department of Materials Science and Engineering, Xi'an Polytechnic University, Xi'an, Shaanxi, 710048, China*

[2]*Department of Textile Science and Engineering, Xi'an Polytechnic University, Xi'an, Shaanxi, 710048, China*

Received 14 September 2023; Received in revised form 3 February 2024; Accepted 6 March 2024

Abstract

In this study, a facile in situ sintering method has been proposed for fabricating high strength lightweight mullite whisker network reinforced proppants. The effect of TiO_2 on the microstructure, properties and fracture behaviours of the mullite whisker network was researched in detail. The addition of TiO_2 promoted the formation of a modified mullite whisker network structure, which effectively improved the flexural strength. The sample containing 4 wt.% TiO_2 exhibited an excellent flexural strength of 215.25 MPa and low bulk density of 1.53 g/cm^3 at 1400 °C. The TiO_2-added mullite whiskers mostly exhibited rod-like crystals with about 0.5–0.8 μm in diameter and 10–15 μm in length. The as-prepared ceramic proppant showed excellent properties, such as low breakage ratio (2.19% under 52 MPa), low density (1.36 g/cm^3) and low acid solubility (2.28 wt.%).

Keywords: *mullite, fracture, strength, sintering, ceramic proppant*

I. Introduction

Hydraulic fracturing is a key technology during the production of unconventional oil and gas wells [1,2]. Proppant is a granular engineering material with certain strength which is widely used in hydraulic fracturing [3,4]. At present, proppants usually can be divided into three types: natural frac sand, ceramic proppants and resin coated proppants [5–7]. Furthermore, in terms of their density, proppants can be divided into three categories as high density, intermediate density and low density [8]. Ideal proppants, as required in hydraulic fracturing processes, have a low density, low cost, high conductivity and high strength [9]. Hence, ceramic proppants have attracted much attention due to their high strength. Moreover, a low density ceramic proppant is desirable because it can avoid sedimentation in a lower viscosity fracturing fluid and increase propped length [10,11].

In the past few decades, ceramic proppant was usually prepared by sintering of high-grade bauxite (>60 wt.% Al_2O_3) in China. The main crystalline phase of these proppants is corundum. The bulk corundum in these proppants can provide sufficient strength. However, high-grade bauxites are expensive and the sintering temperatures of most ceramic proppants are often over 1400 °C. Significant funding and energy are required every year in China for the production of ceramic proppants. Thus, it is necessary to study a method for the preparation of ceramic proppants from low-cost raw materials at low sintering temperatures.

Mullite ($3\,Al_2O_3 \cdot 2\,SiO_2$) has been widely used as engineering ceramic material owing to its high strength, high temperature stability and corrosion resistance [12,13]. Therefore, mullite can be considered as a potential proppant material. Nowadays, there are many methods reported to prepare mullite ceramics, such as molten salt [14], sol-gel [15], mineral decomposition [16], *in situ* [17] and oxide doping methods [18]. The principal problem is to prepare a low-cost, low-density and high strength mullite ceramic material for proppant production. In order to reduce the cost of the preparation of mullite, many researches have been carried out to synthesize mullite from mineral raw materials, such as kyanite [19], coal fly ash [20,21], kaolin [22] and bauxite [23]. Recently, significant work has been conducted on the preparation of porous mullite ceramics from coal fly ash. For example, Dong *et al.* [24] prepared porous

*Corresponding author: tel: +86 15029355851
e-mail: *chenxudong@xpu.edu.cn*

mullite ceramic membranes from coal fly ash and bauxite by dry pressing and sintering process. Cao *et al.* [25] fabricated porous mullite ceramic membrane supports from coal fly ash with the addition of V_2O_5 and AlF_3. Huo *et al.* [26] synthesized high porosity mullite ceramic foams in the range of 73–81% using coal fly ash as the only raw material. However, few studies have been reported on the high strength lightweight mullite ceramics.

Coal gangue is an industrial solid waste produced during coal production (about 10–15% of coal production), which contains Al_2O_3 and SiO_2 as main chemical components [27,28]. It has been reported that the production of coal gangue has reached more than 200 million tons per year in China [29]. Therefore, the comprehensive utilization of such a large quantity of solid waste to reduce the pollution of the environment has become an urgent task [30]. Since the chemical composition of coal gangue is similar to coal fly ash, one important potential application of coal gangue is to prepare mullite ceramics. Previous studies reported that porous mullite ceramic membranes can be prepared by reusing coal gangue [31]. To date, several additives such as AlF_3 [32,33], WO_3 [34], MgO [35], MoO_3 [36] and V_2O_5 [37], have been adopted to decrease the sintering temperature of porous mullite ceramics. Although these sintering additives can promote mullite formation significantly at a lower temperature, they are less effective to improve the strength of mullite ceramics. Generally, the flexural strengths of the porous mullite ceramic membranes were 50–100 MPa [24–28,31]. This strength value should be improved for some advanced structural applications which require high strength lightweight material [38,39]. However, to the best of our knowledge, there are few reports on reusing solid waste coal gangue in preparation of high strength lightweight mullite whisker network. It has been reported that achieving a high degree of secondary mullite interlocked structure with rod-like crystal shape may improve the mechanical properties of ceramics [40]. Therefore, it is very essential to select a suitable sintering additive in order to promote formation of secondary mullite network with improved mullite crystals having good mechanical properties. Previous studies have found that TiO_2 can be used as a nucleation agent to control the crystallization rate in several glassy systems [41,42]. However, few studies have investigated the effect of TiO_2 addition on the microstructure, mechanical properties and acid solubility of mullite whisker network reinforced ceramic proppants.

The main purpose of this work was to obtain high strength lightweight network composed mainly of mullite whiskers appropriate for preparation of ceramic proppants. High strength lightweight mullite whisker network structure was fabricated from coal gangue, bauxite, dolomite, feldspar and TiO_2 by a direct sintering method at relatively low temperature. The effects of adding TiO_2 on the density, flexural strength, fracture behaviours and microstructure of the mullite whisker network were investigated in detail. Furthermore, the optimal mullite whisker network reinforced ceramic material was used to prepare the ceramic proppants. The bulk density, breakage ratio and acid solubility of the mullite whisker network reinforced ceramic proppants were thoroughly investigated.

II. Experimental

2.1. Starting materials

Coal gangue (Datong City, China) and bauxite (Gongyi City, China) were used as the main starting materials. Feldspar (Hohhot City, China), dolomite (Xinzhou City, China) and TiO_2 (99.8%, average particle size of about 25 nm, Sinopharm Chemical Reagent Beijing Co. Ltd, China) were used as sintering additives. Chemical compositions of the starting materials used in the present research are showed in Table 1.

2.2. Preparation

The compositions of the designed samples in this study were shown in Table 2. About 200 g the designed samples and 180 ml water were mixed and homogenized by ball milling for 1 h. Subsequently, the mixture was filtered through 120 mesh. After sufficient drying and screening, the powders were filtered through 120 mesh and pressed into cuboid compacts with a size of 50 mm × 10 mm × 5 mm under die pressing of 20 MPa. The samples were dried at 120 °C for 1 h to remove the excess water and then sintered to 1250–1450 °C in a muffle furnace. The heating rates were 10 °C/min from room temperature to 1250 °C and 2 °C/min up to the final firing temperatures.

Table 2. Designed composition

Sample	Composition [wt.%]				
	Coal gangue	Bauxite	Feldspar	Dolomite	TiO_2
ST-0	72	20	4	4	0
ST-2	70	20	4	4	2
ST-4	68	20	4	4	4
ST-6	66	20	4	4	6

Table 1. Chemical composition of starting materials

Materials	Chemical composition [wt.%]								
	SiO_2	Al_2O_3	Fe_2O_3	TiO_2	CaO	MgO	K_2O	Na_2O	L.O.I.
Coal gangue	48.10	35.06	0.40	0.30	0.26	0.37	0.04	0.02	14.4
Bauxite	12.59	64.07	1.66	2.75	0.12	0.24	1.27	0.21	13.51
Feldspar	70.14	13.59	0.72	0.87	0.55	0.02	9.90	3.22	0.68
Dolomite	0	1.08	0.22	0	31.28	21.05	0	0	45.47

Ceramic proppants were prepared in the following way: the starting materials and water were milled together according to the desired proportions by a planetary high-energy ball mill for 1 h. Then, the mud was filtered through an 80 mesh sieve. Next, the homogeneous mixture was dried in blast drying oven at 120 °C. Spherical green bodies with the desired size (16–30 mesh) were obtained in a sugar-film coating machine (BY-300, Tian tai, China). The spherical green bodies were sufficiently dried at 120 °C, sintered in the same firing process as the previous mullite whisker network reinforced ceramics. After being cooled in air, the ceramic proppants of appropriate size (20–40 mesh) were sieved and tested.

2.3. *Characterization and test*

The chemical compositions of the starting materials were analysed using rapid multi-element analyser (DHF82, China). The bulk densities of sintered samples were measured by the Archimedes' method and calculated by the following formula: $\rho = M/V$, where M is the weight of specimens and V is the volume of specimens. Flexural strength (three-point bending) of the fired samples was obtained by a strength tester (model no. 401/3, Germany). The type of crystalline phases of the sintered samples was identified by an X-ray diffraction (D/Max-2200PC, Rigaku, Japan) with a Cu K_α radiation. The samples were scanned at a scanning rate of 4.0 °/min in the 2θ range from 15° to 70°. Microstructures of the sintered samples were observed using SEM (scanning electron microscope, JSM-6390A, JEOL, Japan). In order to view mullite crystals, the fractured samples were etched in hydrochloric-hydrofluoric acid solution (12 wt.% HCl + 3 wt.% HF) for 20 min and gold coated before their examination by SEM.

The breakage ratio and acid solubility of the mullite whisker network reinforced ceramic proppants were determined according to the Chinese Petroleum and Gas Industry Standard (SY/T 5108-2014). The breakage ratio of the ceramic proppant samples was calculated by the following formula: $W = W_p/W_s \times 100\%$, where W_p is the weight of the samples after crush while W_s is the weight of ceramic proppant samples before crush test. Acid solubility test was performed in hydrochloric-hydrofluoric acid solution (12 wt.% HCl + 3 wt.% HF) at 66 °C for 0.5 h without stir. Acid solubility of the ceramic proppant samples was calculated by the following formula: $S = (M_s + M_r - M_{sr})/M_s \times 100\%$. S is the acid solubility, M_s is the initial weight of ceramic proppant samples before acid solubility test, M_r is the weight of the filter and M_{sr} is the weight of filter containing ceramic proppant samples after the acid solubility test.

III. Results and discussion

XRD patterns of the sintered mullite samples with different TiO_2 additions are shown in Fig. 1. Mullite was observed as the main crystalline phase, and all diffraction peaks can be perfectly matched to mullite. The intensities of mullite peaks increase sharply when TiO_2 content increases from 0 to 2 wt.%. With further increasing TiO_2 content from 4 to 6 wt.%, the peak intensities of the mullite continue a trend of increasing. This indicates that TiO_2 has a significant positive effect on the crystallization of mullite at a low temperature. In addition, feldspar and dolomite are known as efficient fluxes to lower the sintering temperature of mullite [20,35]. Thus, the appropriate content of TiO_2, feldspar and dolomite can have a synergistic effect in reducing the sintering temperature of mullite.

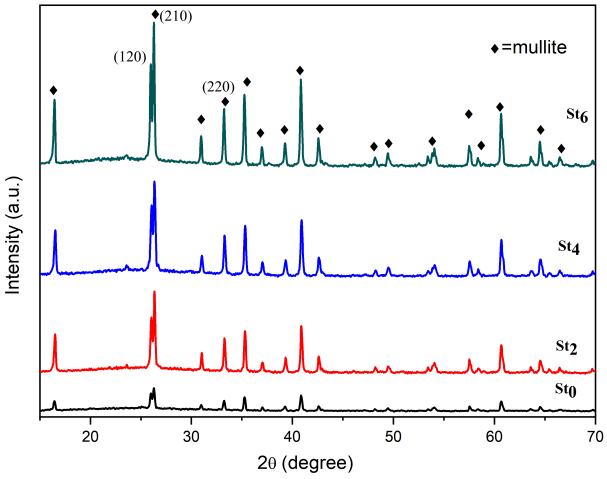

Figure 1. XRD patterns of the samples sintered at 1400 °C

SEM images of the sintered samples (Fig. 2) confirm the formation of two main forms of mullites after sintering process. The one is cuboidal primary mullite with low aspect ratio (1–3 : 1) formed from decomposition of bauxite at lower temperature (<1200 °C). The other is acicular secondary mullite with high aspect ratio (3–10 : 1) formed from the reaction between Al_2O_3 and SiO_2 at higher temperature [43–45]. The microstructure of the samples was influenced by the addition of TiO_2. Some of the large pores and acicular secondary mullite crystals are generally observed in the sample without TiO_2 (Fig. 2a). When 2 wt.% TiO_2 was added to the raw materials, mullite whiskers grew up in the samples and the amount and the size of pores obviously decreased (Fig. 2b). This indicates that the growth of elongated secondary mullite crystals is promoted with the addition of TiO_2. It can be explained by the fact that the addition of TiO_2 reduces the viscosity of the reaction system. Therefore, nucleation of secondary mullite is promoted. In the sample with 4 wt.% TiO_2, the network structure was composed of compact rod-like whiskers which were about 0.5–0.8 μm in diameter and 10–15 μm in length (Fig. 2c). The firm rod-like mullite whiskers skeleton was beneficial for forming a high strength lightweight ceramics [20,38]. When 6 wt.% TiO_2 was added, the columnar form whiskers showed clear adhesions (Fig. 2d). The excess of TiO_2 would produce excess glass phase in the samples, which can lead to bonding of the mullite whiskers.

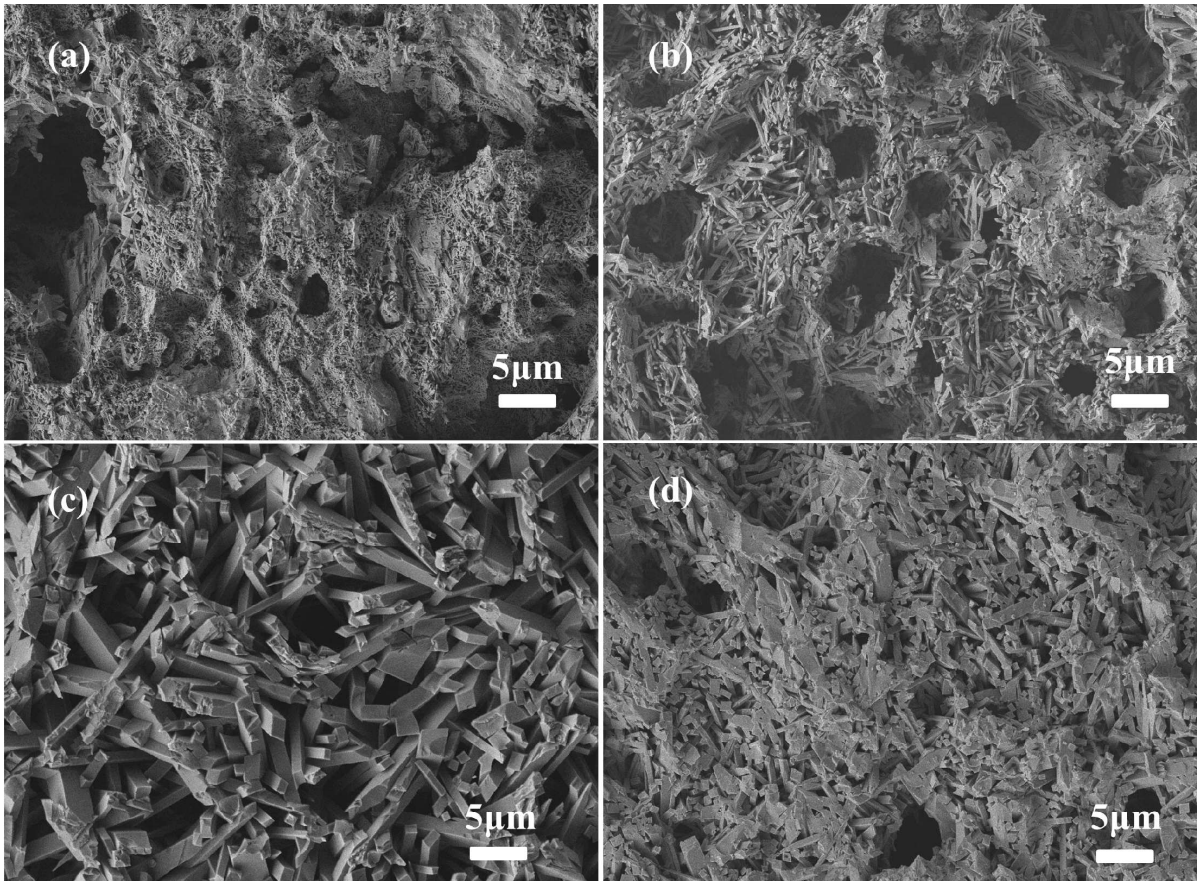

Figure 2. SEM micrographs of the sintered mullite samples with different amount of TiO_2: a) 0 wt.%, b) 2 wt.%, c) 4 wt.% and d) 6 wt.%

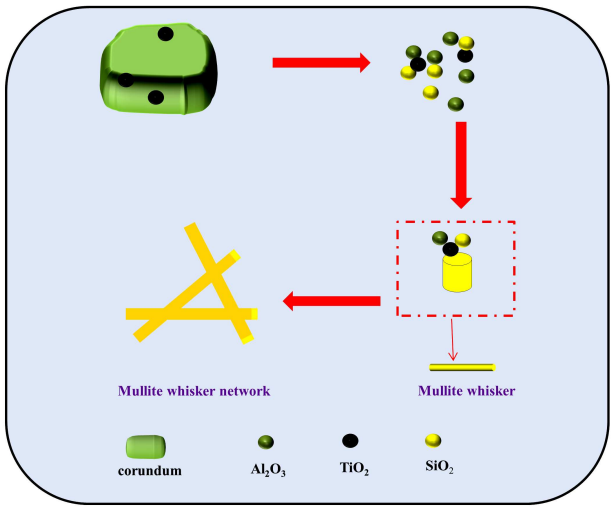

Figure 3. Formation mechanism of mullite whisker network

Figure 3 shows the formation mechanism of mullite whisker network. Firstly, glassy phase is mainly formed from the molten SiO_2 and impurities in the coal gangue and bauxite [46–48]. It is accompanied with transformation of corundum to Al_2O_3 in a low viscosity glasses. Secondly, mullite whiskers crystallize and grow on the surface of TiO_2. Thirdly, mullite whiskers grow continuously and form a mullite whisker network. Previous work has reported the effect of TiO_2 on the viscosity of glasses [40]. It can be explained that the additive of TiO_2 decreases the viscosity in the contact area between corundum relicts and feldspar melted grains [49,50]. Moreover, the alkali and alkaline-earth metal oxides (K_2O, CaO, MgO, etc.) also play an important role in lowering the viscosity of the glassy phase [51]. Meanwhile, TiO_2 is also a good nucleation agent which will increase the crystallization rate of secondary mullite [52]. Thus, the formation of secondary mullite whisker network will effectively be promoted by the presence of TiO_2.

Figure 4 shows the SEM images of the fracture section of the sintered samples. The sample without TiO_2 (Fig. 4a) exhibited an irregular crystal surface. It can be seen that larger and smooth rod-like secondary mullite crystals are more evident in the sample containing 2 wt.% TiO_2 (Fig. 4b). When increasing TiO_2 content to 4 wt.%, all crystals showed a rectangular shape with a smooth surface (Fig. 4c). Therefore, the formation of larger amounts of rod-like secondary mullite must be promoted by the presence of TiO_2. In addition, when comparing the M_2 fracture section (Fig. 4c) with M_1 (Fig. 4a), M_1 was smoother. As shown in Fig. 4c, some cracks dispersed along the crystallographic *c*-axis direction of well-developed mullite whisker, implying that the TiO_2 played an important role in hindering the crack propagation in loading direction in flexural strength test. Bonded crystals and more smooth fracture sections of

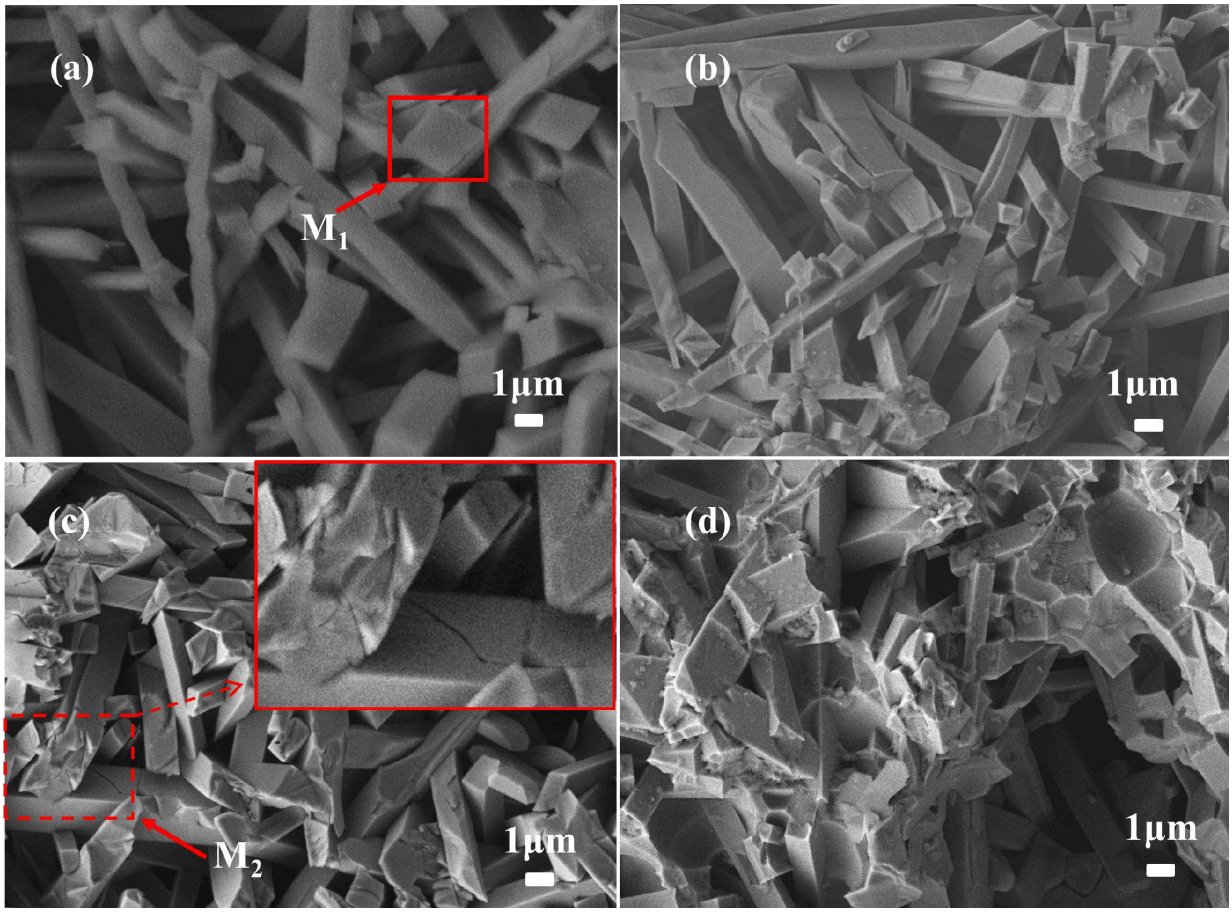

Figure 4. SEM micrographs of the fracture section of the sintered mullite samples with different amount of TiO_2: a) 0 wt.%, b) 2 wt.%, c) 4 wt.% and d) 6 wt.%

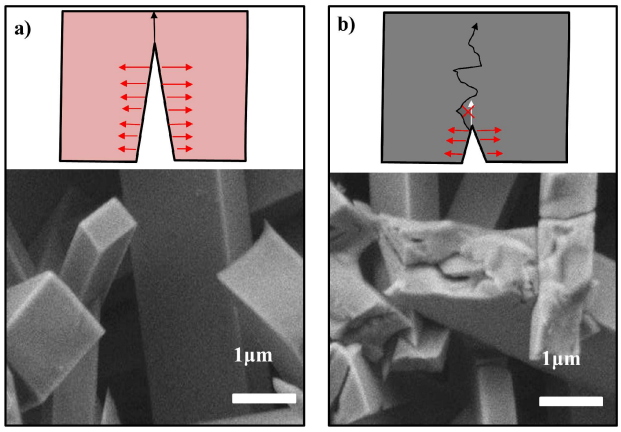

Figure 5. Schematic illustrations of the crack on the fracture section of mullite whisker: a) 0 wt.% and b) 4 wt.% TiO_2

mullite whiskers were obtained in the mullite sample with 6 wt.% TiO_2 (Fig. 4d). Excessive TiO_2 addition resulted in a deformed mullite whisker network and some large pores appeared as seen in Fig. 4d. Thus, it indicated that the appropriate amount of TiO_2 can promote the formation of stronger mullite whiskers and interlocking mullite whisker network structure which could effectively increase the flexural strength [53].

The addition of TiO_2 to the mullite sample strongly modified its fracture behaviour, as it can be seen in Fig. 5. Due to the lack of cracks that spread from one side of the mullite whiskers to another, the surfaces are straight and continuous (Fig. 5a). By contrast, with 4 wt.% TiO_2 addition, the mullite whiskers are refined and the crystal boundaries are increased, causing the deflection of crack as it spreads in mullite crystals (Fig. 5b). The presence of TiO_2 enhanced interfacial layer, provided denser network structure and gave rise to a higher strength of mullite crystals which led to the above observations.

Figure 6 shows fracture mechanism of mullite whisker network. From the results presented in above SEM images, a two-stage mechanistic model for fracture cracking during three-point bending flexural test (as illustrated in Fig. 6a) is proposed. In the first stage, cracks propagate in glass phase (Fig. 6b). When cracks propagate to the cross point of mullite whiskers (as highlight by the red circle in Fig. 6b), the driving force for crack propagation is scattered in different directions. Due to a large amount of energy consumption in that process, crack in loading direction was dramatically weakened. At the second stage, cracks propagate inside the single mullite whisker (Fig. 6c). It is well known that a crack would initiate and propagate at the weakest point. Thus, cracks would change direction and generate quadratic crack when propagating to the points modified by TiO_2 (Fig. 6d). In summary, the selectivity of the direction of crack propagation in the network structure

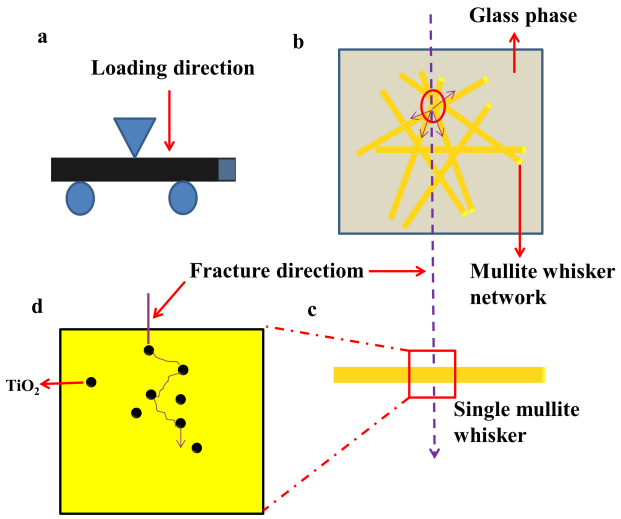

Figure 6. Fracture mechanism schematic diagram of the mullite whisker network: a) schematic view of three-point bending flexural test, b) crack propagation in sintered sample, c) crack propagation in single mullite whisker and d) crack propagation in TiO_2 modified mullite whisker

and the initiation and propagation of quadratic crack consumes a lot of expansion energy, which reduces the crack growth rates. Therefore, appropriate amount of TiO_2 addition results in an improvement in mechanical strength.

Figure 7 illustrates the flexural strength of the mullite samples sintered at various temperatures. The flexural strength of all samples increased sharply in the sintering temperature range from 1200 to 1300 °C. With a content of 4 wt.% TiO_2 (ST-4), the flexural strength also increased significantly at higher sintering temperature, i.e. in the range from 1300 to 1400 °C, and maximal value (215.25 MPa) was achieved at 1400 °C. However, with 6 wt.% TiO_2 addition (ST-6), the flexural strength decreased when sintering temperature was raised from 1300 to 1450 °C. Similar results are also found for sillimanite [54]. This decrease in flexural strength was mainly attributed to excessive amounts of TiO_2 which generated larger pores and deformed mullite whisker network as evidently shown in Figs. 2d and 4d. This clearly indicated negative role of excessive sintering temperature on the flexural strength.

Figure 8 shows the variation in water absorption of the mullite samples sintered at different temperatures. As the quantity of TiO_2 added to the mullite samples increased, a decreasing trend of the water absorption with sintering temperature was observed. At 1350 °C, comparing the result of ST-0 with ST-4, the water absorption of the sample ST-4 with 4 wt.% TiO_2 was sharply reduced. This may be a result of the TiO_2 lowering the viscosity of the glass phase, which flowed easily to fill up the pores [55]. At 1400 °C, water absorption of the ST-4 sample with 4 wt.% TiO_2 was around 0.15% and this indicates almost full density at this temperature.

Figure 9 shows the variation of the bulk density with sintering temperatures for the sample ST-4. The bulk density increased significantly from 1200 to 1400 °C. However, from 1400 to 1450 °C, the density increased

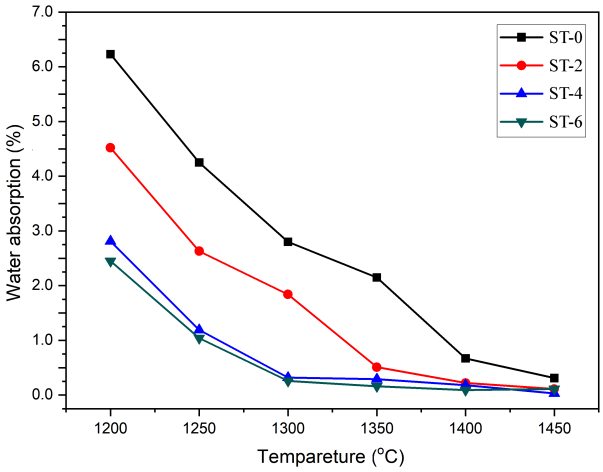

Figure 8. Effect of TiO_2 addition on the water absorption of mullite samples sintered at various temperatures

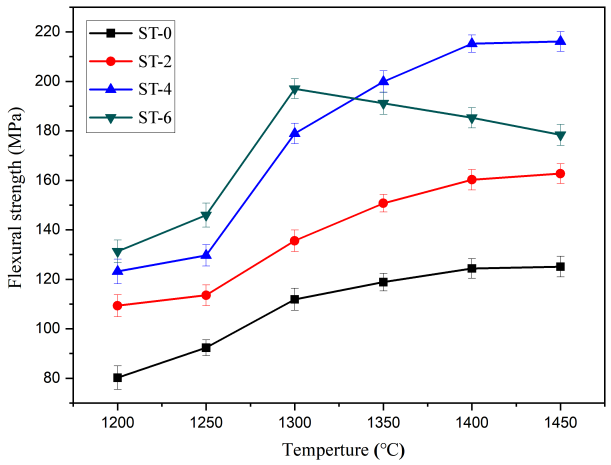

Figure 7. Effect of TiO_2 addition on the flexural strength of mullite samples sintered at various temperatures

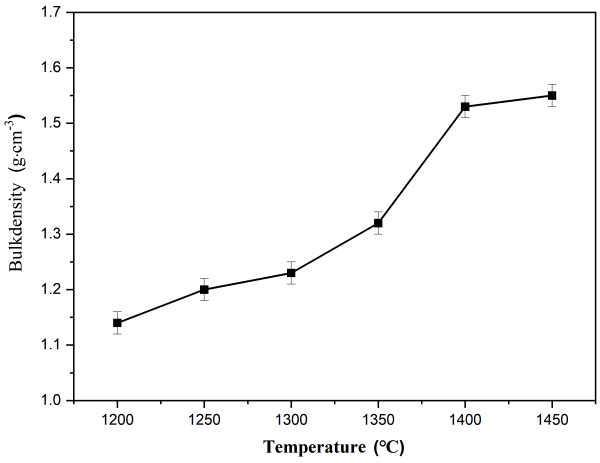

Figure 9. Bulk density of mullite ST-4 sample sintered at various temperatures

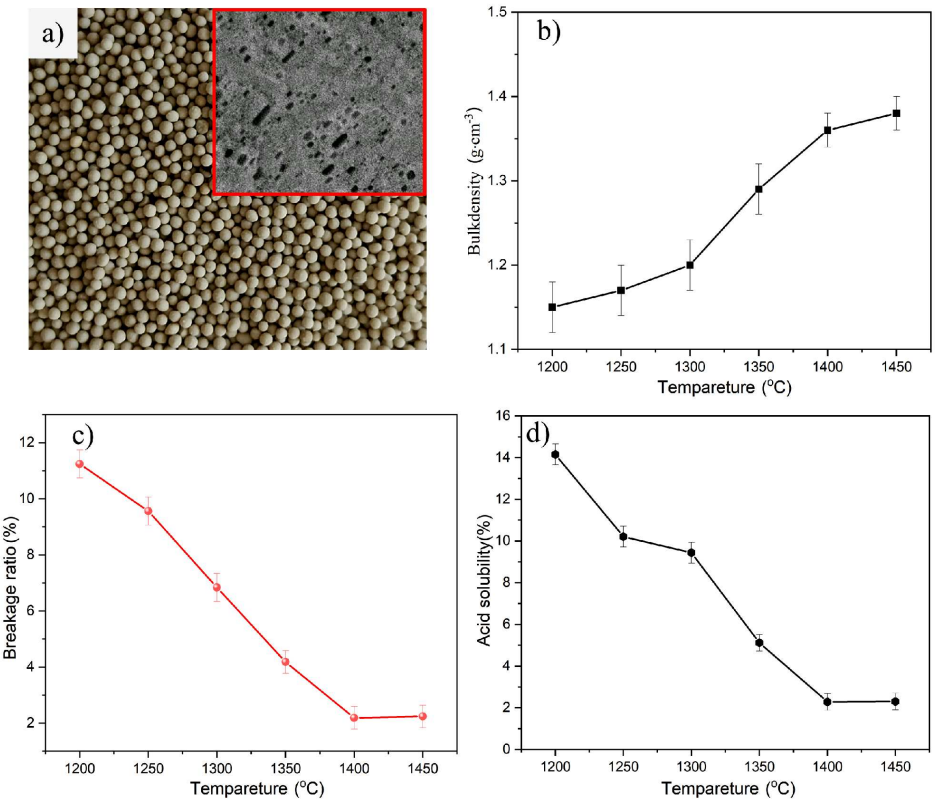

Figure 10. Photo of ceramic proppants (a) and properties of proppants prepared from ST-4 sintered at different temperatures: bulk density (b), breakage ratio - under 52 MPa (c) and acid solubility (d)

relatively slowly, which indicated that significant densification was already obtained. At 1400 °C, the bulk density of sample ST-4 was 1.53 g/cm^3. It is clear that the addition of TiO_2 results in an increase in the bulk density. Promotion of densification process of mullite ceramics with TiO_2 addition can be explained as follows: i) TiO_2 promoted the formation of cation vacancy by Ti^{4+} replacing Al^{3+}, resulting in increased cation mobility, ii) TiO_2 promoted the formation of a liquid phase to increase the diffusion or mass transport of reactants during sintering [56].

Based on the experimental data in the present study, the sample ST-4 was used to prepare the ceramic proppants. As evidenced by Fig. 10a, the mullite whisker network reinforced ceramic proppants show nearly spherical particles with the smooth surface. A lot of pores can be seen on the fracture surface (insert in Fig. 10a), which is believed to reduce the density of proppants. The bulk densities of the ceramic proppant samples are shown in Fig. 10b. The bulk density presents an increasing trend with the increase of the sintering temperature. The bulk density of the ceramic proppant sample was 1.36 g/cm^3 at 1400 °C. According to the Chinese petroleum and natural gas industry standards SY/T5108-2014 (Table 3), the resulting proppant can be classified as a low-density proppant.

The breakage ratio of the ceramic proppants is shown in Fig. 10c. The breakage ratio decreased sharply at the sintering temperature of 1200–1400 °C and increased slightly when the sintering temperature increased from 1400 to 1450 °C. At 1400 °C, the breakage ratio achieved a minimum of 2.19%.

Acid solubility plays a very important role in the performance of proppant. The Chinese petroleum and natural gas industry standards (SY/T5108-2014) require a loss of less than 7.0 wt.% for the ceramic proppant. The acid solubility of the ceramic proppants is shown in Fig. 10d. The acid solubility shows a decreasing trend with increasing sintering temperature. The lowest acid solubility was 2.28 wt.% at 1400 °C. This can be attributed to the addition of TiO_2 reducing the acid solubility of the ceramic proppant. In the sintering process, $MgCO_3$ (dolomite) can react with TiO_2 to form $MgTi_2O_5$ phase that has good acid resistance. In addition, when the appropriate quantity of TiO_2 was added (Fig. 4c), the size and shape of the mullite whisker in the sample ST-4 were uniform and compact. The uniform and compact structure reduced the contact area between the mullite whisker and the acid solution, therefore reducing the acid solubility [57].

Comparison of the ST-4 proppant properties with other products: i) sand, ii) low-density ceramic proppants produced by Wu *et al.* [58], iii) low-density ceramic proppant from Carbo Company and iv) the required values of Chinese petroleum and natural gas industry standards (SY/T5108-2014) for low-density proppant were given in Table 3. The results indicated that the sample ST-4 had the optimal performance, the lowest density, the lowest breakage ratio and acid solubility, compared to other low-density proppants.

Table 3. Comparison of ST-4 proppant properties with other products, such as: sand, low-density ceramic proppants produced by Wu *et al.* [58], low-density ceramic proppants from Carbo Company and the required value of Chinese petroleum and natural gas industry standards (SY/T5108-2014) for low-density proppants

Sample	Bulk density [g/cm^3]	Breaking ratio [%]	Acid solubility [%]
Sand	1.50	25.6	-
Ceramic proppants [58]	-	5.7	5.0
Carbo econoprop	1.56	2.8	-
ST-4	1.48	2.19	2.28
SY/T5108-2014 [8]	<1.65	<10	<7

IV. Conclusions

The high strength lightweight mullite whisker network structures were prepared by direct sintering coal gangue, bauxite, dolomite and feldspar mixtures assisted with TiO_2. The contents of the added TiO_2 had a significant effect on the microstructure and properties of the mullite whisker network structure. The mullite whisker network with 4 wt.% TiO_2 sintered at 1400 °C composed mainly of mullite crystals with a width of 0.5–0.8 μm and length of up to 10–15 μm. The resultant mullite whisker network structure exhibited excellent properties, such as flexural strength of 215.25 MPa and bulk density of 1.53 g/cm^3.

The mullite whisker network structure endowed the ceramic proppants with superior properties. All the properties of the low-density, high strength and mullite whisker network reinforced ceramic proppants obtained using coal gangue as main raw material reached the standards of SY/T5108-2014. The presented method for obtaining the structure of the mullite whisker network is environmentally friendly and energy-saving and can be used as a simple and efficient approach for the preparation of ceramic proppants.

Acknowledgements: This work was supported by the Research Starting Foundation of Xi'an Polytechnic University (No. 107020464).

References

1. C. Mandar, O. Kulkarni, O. Ozden, "Creating novel granular mixtures as proppants: Insights to shape, size and material considerations", *Mech. Adv. Mater. Struct.*, **24** (2017) 605–614.
2. J. Szymanska, P. Wisniewski, P. Wawulska-Marek, J. Mizera, "Determination of loamy resources impact on granulation of ceramic proppants and their properties", *Appl. Clay Sci.*, **166** (2018) 327–338.
3. A. Mocciaro, M.B. Lombardi, A.N. Scian, "Effect of raw material milling on ceramic proppants properties", *Appl. Clay Sci.*, **153** (2018) 90–94.
4. Z. Liu, J. Zhao, Y. Li, Z. Zeng, J. Mao, Y. Peng, Y. He, "Low-temperature sintering of bauxite-based fracturing proppants containing CaO and MnO_2 additives", *Mater. Lett.*, **171** (2016) 300–303.
5. M. Zoveidavianpoor, A. Gharibi, M. Jaafar, "Experimental characterization of a new high-strength ultra-lightweight composite proppant derived from renewable resources", *J. Petrol. Sci. Eng.*, **170** (2018) 1038–1047.
6. M. El-Kader, M. Abdou, A. Fadl, A. Rabou, O. Desouky, M. El-Shahat, "Novel light-weight glass-ceramic proppants based on frits for hydraulic fracturing process", *Ceram. Int.*, **46** (2020) 1947–1953.
7. W. Liu, X. Xiong, Y. Zhao, C. Liu, Y. Hou, X. Pu, "Preparing high-strength and low-density proppants with oil-based drilling cuttings pyrolysis residues and red mud: Process optimization and sintering mechanism", *Fuel*, **331** (2023) 125777.
8. SY/T5108-2014 Standard, "Measurement of properties of proppants used in hydraulic fracturing and gravel-packing operations", *National Energy Board*, China, 2014.
9. X. Xie, S. Niu, Y. Miao, X. Gao, L. Cheng, F. Gao, "Preparation and properties of resin coated ceramic proppants with ultra light weight and high strength from coal- series kaolin", *Appl. Clay Sci.*, **183** (2019) 105364.
10. K. Han, J. Graser, C. Robert, L. Filho, J. Mclennan, T. Sparks, "Synthesis and microstructural evolution in iron oxide kaolinite based proppant as a function of reducing atmosphere, sintering conditions, and composition", *Ceram. Int.*, **44** (2018) 9976–9983.
11. Z. Liao, X. Li, L. Ge, Z. Yang, J. Zhu, Q. Xue, H. Wang, "Lightweight proppants in unconventional oil and natural gas development: A review", *Sustain. Mater. Techno.*, **33** (2022) e00484.
12. H. Liu, X. Xiong, M. Li, Z. Wang, X. Wang, Y. Ma, L. Yuan, "Fabrication and properties of mullite thermal insulation materials with in-situ synthesized mullite hollow whiskers", *Ceram. Int.*, **46** (2020) 14474–14480.
13. Z. Liu, W. Lian, Y. Liu, J. Zhu, C. Xue, Z. Yang, X. Lin, "Phase formation, microstructure development, and mechanical properties of kaolin-based mullite ceramics added with Fe_2O_3", *Int. J. Appl. Ceram. Technol.*, **18** (2021) 1074–1081.
14. J. Gao, B. Wang, Z. Du, Y. Guo, F. Cheng, "Molten salt synthesis of mullite whiskers entirely derived from fly ash for electronic packaging toughening ceramic applications", *J. Mater. Res. Technol.*, **21** (2022) 3719–3731.
15. L. Chen, Z. Wang, Z. Xue, G. Zhou, S. Wang, "Preparation of mullite ceramics with equiaxial grains from powders synthesized by the sol-gel method", *Ceram. Int.*, **48** (2022) 4754–4762.
16. B. Zhang, J. Ma, J. Ye, Y. Jin, C. Yang, J. Ding, Z. Zhang, Z. Hou, Q. Liu, F. Ye, "Ultra-low cost porous mullite ceramics with excellent dielectric properties and low thermal conductivity fabricated from kaolin for radome applications", *Ceram. Int.*, **45** (2019) 18865–18870.
17. M. Wang, Z. Feng, C. Zhai, J. Zhang, Z. Li, H. Zhang, X. Xu, "Low-temperature in-situ grown mullite whiskers toughened heat-resistant inorganic adhesive", *J. Alloys Compd.*, **836** (2020) 155349.
18. K. Li, S. Ge, G. Yuan, H. Zhang, J. Zhang, J. He, Q.

Jia, S. Zhang, "Effects of V_2O_5 addition on the synthesis of columnar self-reinforced mullite porous ceramics", *Ceram. Int.*, **47** (2021) 11240–11248.
19. H. Guo, W. Li, F. Ye, "Low-cost porous mullite ceramic membrane supports fabricated from kyanite by casting and reaction sintering", *Ceram. Int.*, **42** (2016) 4819–4826.
20. X. Chen, T. Li, Q. Ren, X. Wu, H. Li, A. Dang, T. Zhao, Y. Shang, Y. Zhang, "Mullite whisker network reinforced ceramic with high strength and lightweight", *J. Alloys Compd.*, **700** (2017) 37–42.
21. A. Chen, M. Li, J. Xu, C. Lou, J. Wu, L. Cheng, Y. Shi, C. Li, "High-porosity mullite ceramic foams prepared by selective laser sintering using fly ash hollow spheres as raw materials", *J. Eur. Ceram. Soc.*, **38** (2018) 4553–4559.
22. T. Sahraoui, H. Belhouchet, M. Heraiz, N. Brihi, A. Guermat, "The effects of mechanical activation on the sintering of mullite produced from kaolin and aluminum powder", *Ceram. Int.*, **42** (2016) 12185–12193.
23. M. Yan, Y. Li, Y. Sun, L. Li, S. Tong, J. Sun, "Controllable preparation and synthetic mechanism of mullite from the bauxite with Fe-rich oxide content", *Mater. Chem. Phys.*, **202** (2017) 245–250.
24. Y. Dong, J. Zhou, B. Lin, Y. Wang, S. Wang, L. Miao, Y. Lang, X. Liu, G. Meng, "Reaction sintered porous mineral-based mullite ceramic membrane supports made from recycled materials", *J. Hazard. Mater.*, **172** (2009) 180–186.
25. J. Cao, X. Dong, L. Li, Y. Dong, S. Hampshire, "Recycling of waste fly ash for production of porous mullite ceramic membrane supports with increased porosity", *J. Eur. Ceram. Soc.*, **34** (2014) 3181–3194.
26. W. Huo, X. Zhang, Y. Chen, Y. Lu, J. Liu, S. Yan, J. Wu, J. Yang, "Novel mullite ceramic foams with high porosity and strength using only fly ash hollow spheres as raw material", *J. Eur. Ceram. Soc.*, **38** (2018) 2035–2042.
27. C. Li, J. Wan, H. Sun, L. Li, "Investigation on the activation of coal gangue by a new compound method", *J. Hazard. Mater.*, **179** (2010) 515–520.
28. Y. Gao, H. Huang, W. Tang, X. Liu, X. Yang, J. Zhang, "Preparation and characterization of a novel porous silicate material from coal gangue", *Micro. Meso. Mater.*, **217** (2015) 210–218.
29. H. Ji, M. Fang, Z. Huang, K. Chen, Y. Xu, Y. Liu, J. Huang, "Effect of La_2O_3, additives on the strength and microstructure of mullite ceramics obtained from coal gangue and γ-Al_2O_3", *Ceram. Int.*, **39** (2013) 6841–6846.
30. Y. Liu, J. Qin, L. Lu, J. Xu and X. Su, "Enhanced microwave absorption property of silver decorated biomass ordered porous carbon composite materials with frequency selective surface incorporation", *Int. J. Miner. Metall. Mater.*, **30** (2023) 525–535.
31. Q. Lü, X. Dong, Z. Zhu, Y. Dong, "Environment-oriented low-cost porous mullite ceramic membrane supports fabricated from coal gangue and bauxite", *J. Hazard. Mater.*, **273** (2014) 136–145.
32. M. Rashad, U. Sab, G. Logesh, C. Srishilan, M. Lodhe, A. Joy, M. Balasubramanian, "Mullite phase evolution in clay with hydrated or anhydrous AlF_3", *J. Eur. Ceram. Soc.*, **40** (2020) 5974–5983.
33. S. Fan, H. Zheng, Q. Gao, Y. Li, Y. Chen, G. Liu, B. Fan, R. Zhang, "Preparation of Al_2O_3-mullite thermal insulation materials with AlF_3 and SiC as aids by microwave sintering", *Int. J. Appl. Ceram. Technol.*, **17** (2020) 2250–2258.
34. L. Kong, H. Huang, T. Zhang, J. Ma, F. Boey, R. Zhang, Z. Wang, "Growth of mullite whiskers in mechanochemically activated oxides doped with WO_3", *J. Eur. Ceram. Soc.*, **23** (2003) 2257–2264.
35. Y. Dong, S. Hampshire, J. Zhou, Z. Ji, J. Wang, G. Meng, "Sintering and characterization of fly ash-based mullite with MgO addition", *J. Eur. Ceram. Soc.*, **31** (2011) 687–695.
36. Z. Hou, B. Cui, L. Liu, Q. Liu, "Effect of the different additives on the fabrication of porous kaolin-based mullite ceramics", *Ceram. Int.*, **42** (2016) 17254–17258.
37. J. Li, H. Ma, W. Huang, "Effect of V_2O_5 on the properties of mullite ceramics synthesized from high-aluminum fly ash and bauxite", *J. Hazard. Mater.*, **166** (2009) 1535–1539.
38. X. Chen, T. Li, Q. Ren, X. Wu, A. Dang, H. Li, T. Zhao, "Fabrication and morphology control of high strength lightweight mullite whisker network", *J. Alloys Compd.*, **729** (2017) 285–292.
39. J. Zhao, Z. Liu, Y. Li, "Preparation and characterization of low-density mullite based ceramic proppant by a dynamic sintering method", *Mater. Lett.*, **152** (2015) 72–75.
40. N. Montoya, F. Serrano, M. Reventós, J. Amigo, J. Alarcón, "Effect of TiO_2, on the mullite formation and mechanical properties of alumina porcelain", *J. Eur. Ceram. Soc.*, **30** (2010) 839–846.
41. M. Esmaili, M. Nilforoushan, M. Tayebi, E. Aghaie, "Effect of micro/nano TiO_2 addition on the densification behavior and mechanical properties of multifunctional resistant porcelains", *Ceram. Int.*, **47** (2021) 17435–17444.
42. F. Torres, J. Alarcon, "Microstructural evolution in fast-heated cordierite-based glass-ceramic glazes for ceramic tile", *J. Am. Ceram. Soc.*, **87** (2005) 1227–1232.
43. W. E. Lee, Y. Iqbal, "Influence of mixing on mullite formation in porcelain", *J. Eur. Ceram. Soc.*, **21** (2001) 2583–2586.
44. C. Chen, G. Lan, W. Tuan, "Preparation of mullite by the reaction sintering of kaolinite and alumina", *J. Eur. Ceram. Soc.*, **20** (2000) 2519–2525.
45. H. Lu, W. Wang, W. Tuan, M. Lin, "Acicular mullite crystals in vitrified kaolin", *J. Am. Ceram. Soc.*, **87** (2004) 1843–1847.
46. P. Zhao, S. Ma, X. Wang, W. Wu, Y. Ou, "Properties and mechanism of mullite whisker toughened ceramics", *Ceram. Int.*, **49** (2023) 10238–10248.
47. Y. Chen, G. Liu, Q. Gu, S. Li, B. Fan, R. Zhang, H. Li, "Preparation of corundum-mullite refractories with lightweight, high strength and high thermal shock resistance", *Materialia*, **8** (2019) 100517.
48. Y. Si, S. Fan, H. Wang, M. Xia, L. Li, G. Liu, H. Li, R. Zhang, B. Fan, Y. Chen, "Preparation of lightweight corundum-mullite thermal insulation materials by microwave sintering", *Process. Appl. Ceram.*, **15** (2021) 170–178.
49. P. Behera, S. Bhattacharyya, "Sintering and microstructural study of mullite prepared from kaolinite and reactive alumina: Effect of MgO and TiO_2", *Int. J. Appl. Ceram. Technol.*, **18** (2021) 81–90.
50. E. Sola, F. Serrano, E. Delgado-Pinar, M. Reventós, A. Pardo, M. Kojdecki, "Solubility and microstructural development of TiO_2-containing $3Al_2O_3{\cdot}2SiO_2$ and $2Al_2O_3{\cdot}SiO_2$ mullites obtained from single-phase gels", *J.*

Eur. Ceram. Soc., **27** (2007) 2647–2654.
51. Y. Dong, X. Feng, X. Feng, Y. Ding, X. Liu, G. Meng, "Preparation of low-cost mullite ceramics from natural bauxite and industrial waste fly ash", *J. Alloys Compd.*, **460** (2008) 599–606.
52. M. Rezvani, B. Eftekhari-Yekta, M. Solati-Hashjin, K. Marghussian, "Effect of Cr_2O_3, Fe_2O_3 and TiO_2 nucleants on the crystallization behaviour of SiO_2-Al_2O_3-CaO-MgO(R_2O) glass-ceramics", *Ceram. Int.*, **31** (2005) 75–80.
53. L. Zhu, Y. Dong, S. Hampshire, S. Cerneaux, "Waste-to-resource preparation of a porous ceramic membrane support featuring elongated mullite whiskers with enhanced porosity and permeance", *J. Eur. Ceram. Soc.*, **35** (2015) 711–721.
54. S. Sen, P. Aggarwal, "Effect of TiO_2 and ZrO_2 on sintering of sillimanite", *Ceram. Int.*, **20** (1994) 299–302.
55. H. Fathi, A. Johnson, "The effect of TiO_2 concentration on properties of apatite- mullite glass-ceramics for dental use", *Dent. Mater.*, **32** (2016) 311–322.
56. S. Naga, A. El-Maghraby, "Preparation and characterization of porous fibrous mullite bodies doped with TiO_2", *Mater. Charact.*, **62** (2011) 174–180.
57. T. Wu, J. Zhou, B. Wu, "Effect of TiO_2 content on the acid resistance of a ceramic proppant", *Corros. Sci.*, **98** (2015) 716–724.
58. X. Wu, Z. Hou, Q. Ren, H. Li, F. Lin, T. Wei, "Preparation and characterization of ceramic proppants with low density and high strength using fly ash", *J. Alloys Compd.*, **702** (2017) 442–448.